

INVESTIGATION INTO THE PETROGENESES OF APOLLO 14 HIGH-ALUMINA BASALTIC MELTS THROUGH CRYSTAL STRATIGRAPHY. H. Hui¹, J. G. Oshrin¹, and C. R. Neal¹, ¹Department of Civil Engineering and Geological Sciences, University of Notre Dame, Notre Dame, IN 46556, (hhui@nd.edu, neal.1@nd.edu)

Introduction: The Apollo 14 high-alumina basaltic samples ($\text{Al}_2\text{O}_3 = 11\text{-}16 \text{ wt\%}$) were collected from the Moon's Fra Mauro region, which is composed mostly of impact ejecta from the Imbrium basin and some pristine basalts (and pristine basalt clasts in some breccias). Various models have been proposed for the petrogenesis of the high-Al basalts [1-4]. Using whole-rock trace element ratios unaffected by fractional crystallization of observed phases, Neal and Kramer [4] found that the pristine high-Al basalts formed three different groups (Groups A, B, and C) and an ungrouped sample 14072, thus indicating they were derived from distinct source regions. We further investigate the petrogenetic processes of Apollo 14 high-Al basaltic melts using plagioclase compositions.

Methods: Plagioclase crystals in ten Apollo 14 high-Al basaltic melts are used for compositional analyses: *Electron Microprobe Analysis* for major chemistry, *LA-ICP-MS Analysis* for trace elements [5].

Results and Discussion: Whole-rock compositions of Apollo 14 high-Al basalts suggests Group A basalts could have formed by 30-40% closed-system fractional crystallization (FC), while Group B and C basalts require assimilation of a distinct, evolved composition in conjunction with fractional crystallization (AFC) [4]. Using the plagioclase trace-element data, modeling of AFC scenarios were carried out to determine if the compositional data of this study support these petrogenesis processes.

Partition Coefficients (D_i^{plag}). To deduce the processes that occurred during the magma evolution of each Apollo 14 high-Al basaltic melt, partition coefficients (D_i^{plag}) have to be estimated carefully so that the calculated trace-element concentrations in the melts equilibrated with plagioclase crystals can approach to the actual values during magmatic processes. The dependence of D_i^{plag} on anorthite content of plagioclase has been experimentally verified [e.g., 6, 7] as:

$$RT \ln D_i^{\text{plag}} = a_i X_{\text{An}} + b_i$$

where X_{An} is the anorthite mole percentage in plagioclase, R is the gas constant, T is temperature in K, a_i and b_i are constants deduced from laboratory experiments ($i = \text{Sr, Y, Ba, La, Ce, Nd, Sm, Er, and Yb}$) [7-11]. An average value ($D_{\text{Eu}}^{\text{plag}} = 0.698$) of three data points at $1473 \pm 20 \text{ K}$ and IW buffer in Aigner-Torres et al. [10] was used in modeling petrogeneses. Due to a lack of experimental constraints, an average value for Gallium ($D_{\text{Ga}}^{\text{plag}} = 0.94$) from the partition coefficients

deduced from natural plagioclase crystals with 75-92% of anorthite in terrestrial basalts [12] was used here.

Figure 1 shows comparisons of calculated trace-element concentrations in melts equilibrated with plagioclase crystals using the D_i^{plag} s and whole-rock compositions [4]. In general, the trace elements in the residual melts became enriched as melt crystallization continued during magma evolution.

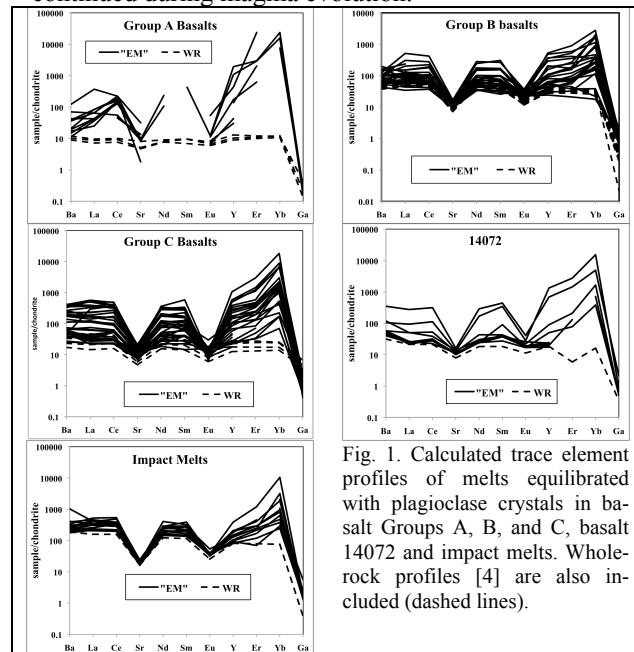


Fig. 1. Calculated trace element profiles of melts equilibrated with plagioclase crystals in basalts Groups A, B, and C, basalt 14072 and impact melts. Whole-rock profiles [4] are also included (dashed lines).

Petrogenesis of Group A Basalts. Whole-rock data suggests that the ranges of trace elements in Group A basalts can be produced by 30 – 40% closed-system FC [4]. This petrogenesis, however, is not reflected in the equilibrium melt conditions recorded by the plagioclase crystals. Figure 2 suggests that plagioclase continued to crystallize beyond 40% total crystallization, and indicates that small amounts of assimilation may have occurred. The solid lines (Fig. 2) represent the model of AFC with an r -value of 0.2 and an assimilant composition of a possible mixture of KREEP and granite. Assimilation may have occurred by entrainment of KREEP/granite-rich material when the magma flowed across the regolith on the lunar surface.

Petrogenesis of Group B Basalts. Most equilibrium melt compositions of Group B basalt fall between the FC trajectory and the AFC trajectory with an r -value of 0.5 (Fig. 2); whole-rock trace-element compositions, on the other hand, would suggest an AFC trajectory with an r -value representing the weighted aver-

age of all r -values experienced during petrogenesis. If the r -value fluctuated during the petrogenesis of the Group B basalts, then the equilibrium melt compositions calculated from different locations on plagioclase crystals would not fall on a single AFC trajectory (Fig. 2). It is also possible that the assimilant composition fluctuated between KREEP and granite during crystallization, which would cause disparities between the whole-rock model [4] and that developed here.

Petrogenesis of Group C Basalts. Most of the equilibrium melt compositions of Group C basalt fall in the region outlined by the AFC trajectory with an r -value of 0.5 and FC trajectory (Fig. 2). The fact that all equilibrium melt compositions do not fall on a single FC or AFC trajectory suggests that, as with the Group B basalts, the r -value fluctuated during crystallization. Furthermore, the fact that the assimilant composition used in this model differs from that used in the modeling of the whole-rock data indicates that the assimilated component may also have varied between KREEP and granite during basalt petrogenesis.

Petrogenesis of Basalt 14072. Sample 14072 is a pristine, but ungrouped basalt. As with the Groups A, B, and C basalts, those of basalt 14072 cannot be explained by closed-system fractional crystallization process or a single trajectory of assimilation and fractional crystallization (Fig. 2). In fact, the petrogenetic model suggests that the *r*-value fluctuated during crystallization. The assimilant composition may also have varied between KREEP and granite during the petrogenesis process of 14072.

Petrogenesis of Impact Melts. In contrast to those of the pristine basalts, the calculated equilibrium melt compositions of plagioclase crystals in the impact melts can be explained by fractional crystallization (Fig. 2). The petrogenesis of impact melts does not require open-system evolution through assimilation. The whole-rock data of impact melt 14310,661 [4] also fall on the FC trajectory (Fig. 2).

Pristine Basalts versus Impact Melts. The compositional micro-heterogeneity in the basalts observed in this study suggests that the high-Al pristine basalts continued to evolve via assimilation and fractional crystallization as they flowed across the lunar surface. The compositional variations displayed in Figs. 1 and 2 may partially result from the following volcanic scenario, which has been observed on Earth [13]. The pristine high-Al basalts crystallized in fast moving lava flows that had open channels connecting the vents to the flow fronts after their emplacement on the lunar surface. As the lava flowed, the cooled lava crust in contact with the lunar regolith was assimilated. This crust contained KREEP/granite-rich clasts from the loose regolith. Thus, the assimilant changed in terms of

both composition (KREEP and/or granite) and mass (r -value) throughout magma crystallization and within individual flows. The low viscosity of lunar basaltic melts comparing to terrestrial basalts [14] can enhance both lava flow and entrainment rates of the crust back into the fluid center of the flow. In contrast, the petrogeneses of impact melts require little assimilation. The composition evolution in the plagioclase crystals of impact melts can be explained by fractional crystallization. Hence, the Apollo 14 impact melts may be solidified in a more static environment, such as the impact-generated melt lake. This scenario indicates a slower cooling rate comparing to the pristine basaltic lava flows. Assimilation of low melting point components (i.e., KREEP and granite) is feasible during lava flowing across the lunar surface, but this would also further accelerate magma cooling by consumption of thermal energy of magma. The cooling rates of pristine basalts and impact melts are consistent with the slopes of their CSD curves from the textural analyses [5].

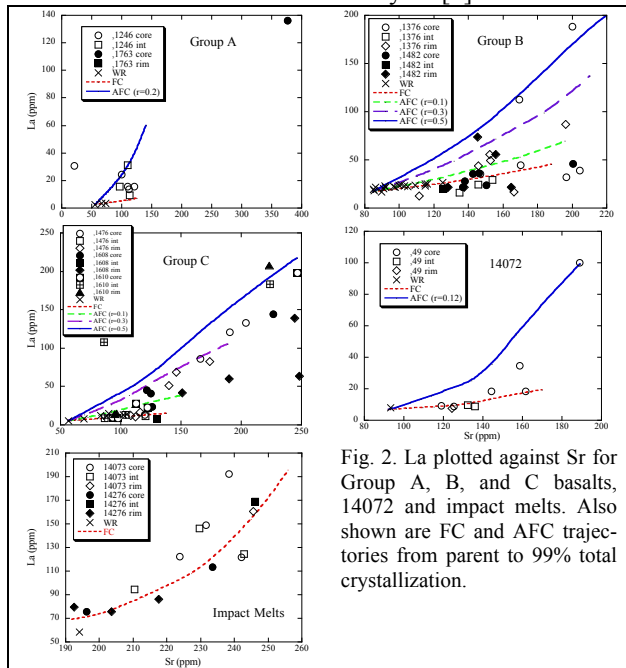


Fig. 2. La plotted against Sr for Group A, B, and C basalts, 14072 and impact melts. Also shown are FC and AFC trajectories from parent to 99% total crystallization.

References: [1] Dickinson T. et al. (1985) *LPS XV*, C365-C374. [2] Shervais J. W. et al. (1985) *LPS XV*, C375-C395. [3] Hagerty J. J. et al. (2005) *GCA*, 69, 5831-5845. [4] Neal C. R. and Kramer G. (2006) *AM*, 91, 1521-1535. [5] Oshrin J. G. and Neal C. R. (2009) *LPS XXXX*, Abstract # 1706. [6] Blundy J. D. and Wood B. J. (1991) *GCA*, 55, 193-209. [7] Bindeman I. N. et al. (1998) *GCA*, 62, 1175-1193. [8] Blundy J. D. (1997) *CG*, 141, 73-92. [9] Bindeman I. N. and Davis A. M. (2000) *GCA*, 64, 2863-2878. [10] Aigner-Torres M. et al. (2007) *CMP*, 153, 647-667. [11] Tepley III F. J. et al. (2010) *Lithos*, 118, 82-94. [12] Goodman R. J. (1972) *GCA*, 36, 303-317. [13] Keszthelyi L. and Self S. (1998) *JGR*, 103, 27447-27464. [14] Murase T. and Mc Birney A. R. (1970) *Science*, 167, 1491-1493.